# Periodic Mesoporous Silica-Supported Recyclable Rhodium-Complexed Dendrimer Catalysts

Jan P. K. Reynhardt, Yong Yang, Abdelhamid Sayari,* and Howard Alper*

*Centre for Catalysis Research and Innovation (CCRI), Department of Chemistry, University of Ottawa, 10 Marie Curie, Ottawa, Ontario, Canada K1N 6N5*

*Received April 29, 2004. Revised Manuscript Received August 3, 2004*

Polyamidoamine (PAMAM) dendrimers up to the third generation were grown for the first time inside the channels of a large-pore (6.5 nm) MCM-41 silica. In-depth characterization of such materials showed that the dendrimers grew inside the channels. The third generation was found to almost completely fill the pore system. The supported dendrimers of generations 0, 1, and 2 were phosphinomethylated and then complexed with rhodium. The G(0) and G(1) materials were found to be very active in olefin hydroformylation. The hydroformylation of 1-octene was accomplished with a turnover frequency of 1800 $h^{-1}$ at 70 °C and the catalyst could be recycled several times without loss in activity.

## Introduction

Dendrimers are nanosized, highly branched molecules with distinct architecture, which provides unprecedented control over structural unit positioning. Synthetic methodologies leading to dendrimers with precisely controlled size, shape, and location of functional groups have been developed. This led to the design of innovative dendritic materials for a variety of advanced applications.[1,2] In particular, when terminated with organometallic complexes, dendrimers grown on solid materials such as resins, polymers beads, or inorganic oxides, e.g. amorphous silica, have attracted much interest in recent years as recyclable heterogenized homogeneous catalysts.[3−10] Alper and co-workers[3−6] carried out extensive work on Rh- and Pd-complexed dendrimers anchored on an amorphous silica with average pore size of 6 nm. These catalysts were found to be highly efficient in terms of activity and regioselectivity and easily recoverable and recyclable. However, even though catalysts based on third- and fourth-generation dendrimers were supposed to exhibit higher density of active sites, they were found to be less effective than catalysts of lower generation. This was attributed to steric crowding,[3] made worse by the irregular nature of the surface of amorphous silica.

To be able to increase the catalyst loading through the use of higher generation dendrimers, it is proposed to use silicas with more appropriate pore structures to circumvent the limitations imposed by the relatively small pore size of amorphous silica used and its irregular pore structure. Periodic mesoporous silicas (PMS) with large pore sizes would be a suitable choice. The regular nature of the pore system of PMS offers a unique opportunity to precisely control the location, density, and growth of dendrimers. Other properties of PMS, such as their high surface area, and their adjustable pore system, in terms of size, shape, and connectivity, offer added flexibility for the design of highly loaded, thus more efficient, catalysts. The combination of ordered large surface area support silica with highly organized dendrimers offers ideal conditions for catalyst spatial design and optimization. The current investigation deals with the synthesis and catalytic properties of different generations of rhodium-complexed polyamidoamine (PAMAM) dendrimers grown inside the channels of MCM-41 silica (Rh−$PPh_2$−PAMAM−MCM-41). In the current investigation, a large pore (6.5 nm) MCM-41 silica prepared by hydrothermal restructuring[11] was selected as support for two reasons: (i) the pore is large enough to accommodate higher dendrimer generations and (ii) such materials exhibit enhanced stability.[12]

## Experimental Section

**Synthesis of Large-Pore MCM-41.** Large pore MCM-41 silica was prepared in the presence of cetyltrimethylammonium bromide (CTAB) via the pore expansion method first reported by Khushalani et al.[13] and further developed by our group.[11,12,14,15] The synthesis mixture had the following molar

* Corresponding authors. E-mail: abdel.sayari@science.uottawa.ca, halper@science.uottawa.ca.

(1) Diez-Barra, E.; Garcia-Martinez, J. C.; del Rey, R.; Rodriguez-Lopez, J.; Giacalone, F.; Segura, J. L.; Martin, N. *J. Org. Chem.* **2003**, *68*, 3178 and references therein.
(2) Minard-Basquin, C.; Weil, T.; Hohner, A.; Radler, J. O.; Mullen, K. *J. Am. Chem. Soc.* **2003**, *125*, 5832.
(3) Bourque, S. C.; Alper, H.; Manzer, L. E.; Arya, P. *J. Am. Chem. Soc.* **2000**, *122*, 956.
(4) Bourque, S. C.; Maltais, F.; Xiao, W.-J.; Tardif, O.; Alper, H.; Arya, P.; Manzer, L. E. *J. Am. Chem. Soc.* **1999**, *121*, 3035.
(5) Antebi, S.; Arya, P.; Manzer, L. E.; Alper, H. *J. Org. Chem.* **2002**, *67*, 6623.
(6) Reynhardt, J. P. K.; Alper, H. *J. Org. Chem.* **2003**, *68*, 8353.
(7) Arya, P.; Panda, G.; Rao, N. V.; Alper, H.; Bourque, S. C.; Manzer, L. E. *J. Am. Chem. Soc.* **2001**, *123*, 2889.
(8) Lu, S.-M.; Alper, H. J. *Am. Chem. Soc.* **2003**, *125*, 13126.
(9) (a) Dahan, A.; Portnoy, M. *Org. Lett.* **2003**, *5*, 1197. (b) Dahan, A.; Portnoy, M. *Chem. Commun.* **2002**, 2700.
(10) Chung, Y. M.; Rhee, H. K. *Chem. Commun.* **2002**, 238.
(11) Sayari, A.; Liu, P.; Kruk, M.; Jaroniec, M. *Chem. Mater.* **1997**, *9*, 2499.
(12) Kruk, M.; Jaroniec, M.; Sayari, A. *J. Phys. Chem. B.* **1999**, *103*, 4590.
(13) Khushalani, D.; Kuperman, A.; Ozin, G. A.; Tanaka, K.; Garces, J.; Olken, J. J.; Coombs, N. *Adv. Mater.* **1995**, *7*, 842.
(14) Kruk, M.; Jaroniec, M.; Sayari, A. *Langmuir* **1997**, *13*, 6267.

10.1021/cm0493142 CCC: $27.50 
Published on Web 09/18/2004

**Scheme 1. Structure of Generations 0−3 of Silica-Supported PAMAM Dendrimers**

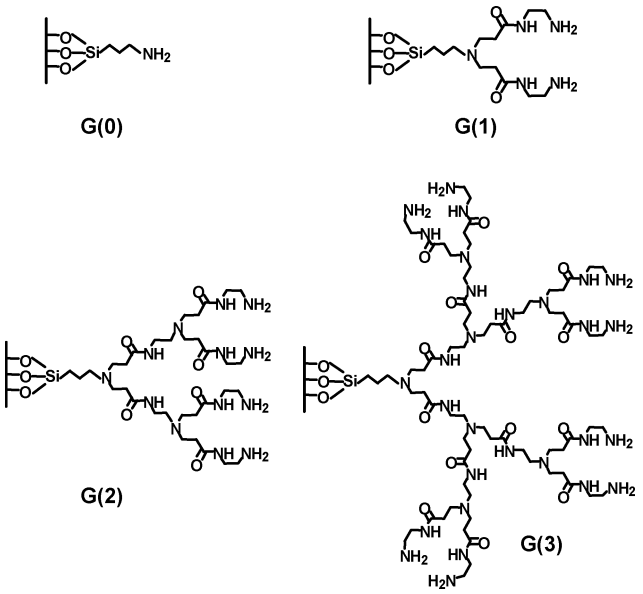


composition 1:0.33:0.17:0.17:17 $SiO_2$:TMAOH:CTAB:$NH_4$-OH:$H_2O$. Fumed Cab-O-Sil M-5 silica (36 g) was suspended in water (60 g) under vigorous stirring, and then 61.6 g of 25 wt % tetramethylammonium hydroxide (TMAOH) was added. Independently, 36.5 g of CTAB was dissolved in 65.6 g of water, and subsequently 11.7 g of 30 wt % $NH_4OH$ was introduced. The mixtures containing the silica and CTAB were stirred together for ca. 30 min and then transferred into a Teflon-lined autoclave and treated under autogenous pressure without stirring at 343 K for 3 days. Subsequently, the autoclave was transferred in another oven preheated at 150 °C and kept for 24 h. The obtained material was filtered, washed, dried, and calcined at 540 °C for 5 h under flowing air (6 L/h).

**Propylamine Grafting.** This was performed in a three-necked round flask under nitrogen. Calcined MCM-41 (10 g) was first dried at 120 °C for 2 h to remove surface humidity and then added into 200 mL of boiling anhydrous toluene. After 1 h of stirring and refluxing, 4.82 g of 3-aminopropyl-triethoxysilane (APTES) was added to this mixture, which was then stirred and refluxed at 110 °C for 5 h. The white amine-functionalized MCM-41 was separated by filtration, thoroughly washed with toluene, and dried in ambient condition.

Preparation and Characterization of Dendrimers Supported on Mesoporous Materials. Polyamidoamine (PAMAM) dendrimers, up to the third generation (Scheme 1) were prepared using a modified multistep procedure based on literature methods[3] (Scheme 2), on amine-modified large pore MCM-41. Samples will be referred to as G(*x*), where *x* is the number of the dendrimer generation. The starting MCM-41 material will be designated as G(−0.5), and the propylamine-modified material as G(0). The synthesis of G(0.5) was as follows. Aminopropyl-functionalized MCM-41 (6.9 mmol $NH_2$, 6 g) and methyl acrylate (0.14 mol, 11.82 g) were stirred at 50 °C in dry methanol (300 mL) under a nitrogen atmosphere for 5 days. The mixture was cooled and filtered through a medium-pore frit under nitrogen flow and washed with dry methanol (3 × 50 mL). The residual solvent was removed in vacuo, affording methyl propylaminopropionate-functionalized MCM-41 in 98% yield.

Supported G(1) dendrimer was prepared as follows. Methyl propylaminopropionate-functionalized MCM-41 (0.13 mol ester groups, 6 g) was added to ethylenediamine (65 mL) in dry methanol (300 mL) under a nitrogen atmosphere. The reaction was stirred for 5 days and the resulting G(1) dendrimer

**Scheme 2. Preparation of MCM-41 Silica-Supported Dendrimers**

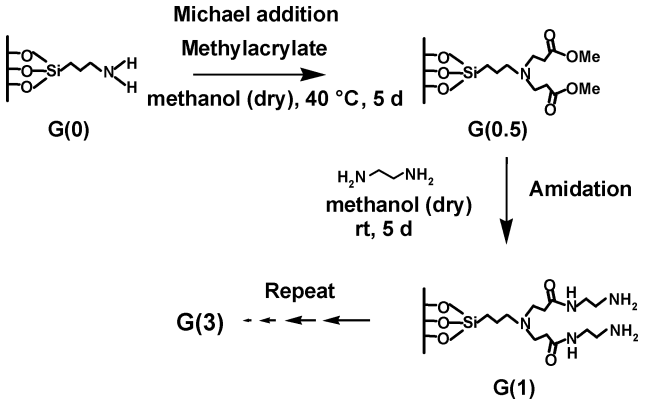


**Scheme 3. Rh-G(0) Catalyst**

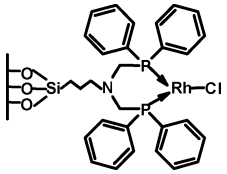

supported on MCM-41 was isolated by filtration through a medium-pore frit. The solid was washed with dry methanol (3 × 50 mL), and the residual solvent was removed in vacuo. The higher generations were prepared by repetition of the two steps described above, the amount of reagents being adjusted as required.

**Phosphinomethylation of Dendrimers.** The dendrimers were phosphinomethylated using diphenylphosphine and paraformaldehyde by modification of the literature method.[16] The double phosphinomethylation of the terminal amine groups of the dendrimers was achieved by reacting the dendrimers with diphenylphosphinomethanol prepared in situ from diphenylphosphine and paraformaldehyde in toluene (110 °C, 48 h).

The actual procedure was as follows. To a stirred suspension of paraformaldehyde (0.84 equiv, 1.36 g) in dry toluene (20 mL) under argon was added diphenylphosphine (0.054 mol, 10 g). The resulting mixture was heated to reflux (110 °C) and stirred for 2 h until the mixture became clear. At this stage, aminopropyl-functionalized MCM-41 (2.9 mmol $NH_2$, 2.5 g) was added and the resulting suspension was stirred under argon at reflux (110 °C) for 48 h. The phosphinomethylated aminopropyl-functionalized MCM-41 was isolated by filtration through a medium-pore frit under a flow of argon, and the resulting light yellow solid was washed with toluene (2 × 20 mL). The residual solvent was removed in vacuo. Phosphinomethylated materials will be referred to as P-G(*x*).

**Complexation of the Phosphinomethylated Dendrimers.** The phosphinomethylated dendrimers were readily complexed (Scheme 3) on treatment with the appropriate rhodium complexes in toluene (rt, 1−2 h under argon). The support turned yellow and decolorization of the supernatant solvent was used as an indication of the extent of complexation. The detailed procedure was as follows. Phosphinomethylated aminopropyl-functionalized MCM-41 (0.82 mmol $PPh_2$, 1 g) and $[Rh(COD)Cl]_2$ (0.204 mmol, 0.1006 g) were stirred under argon for 2 h in dry toluene (20 mL). The mixture was filtered through a medium-pore frit under argon flow and washed with toluene (2 × 20 mL). The residual solvent was removed in vacuo to yield the product. The complex was stored under argon. These materials will be designated Rh-G(*x*).

**Characterization.** X-ray powder diffraction (XRD) patterns were collected on a Scintag $X_2$ Advanced Diffraction System

(15) Kruk, M.; Jaroniec, M.; Sayari, A. *Microporous Mesoporous Mater.* **1997**, *27*, 217.

(16) Reetz, M. T.; Lohmer, G.; Schwickardi, R. *Angew. Chem., Int. Ed. Engl.* **1997**, *36*, 1526.

**Scheme 4. Hydroformylation Reaction**

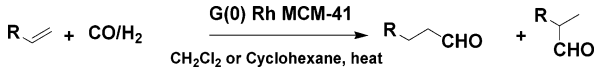


using Cu Kα radiation with 0.15418 nm wavelength, a step size of 0.02° 2$\theta$, and a counting time per step of 4.0 s over a 0.7° < 2$\theta$ < 8° range. Nitrogen adsorption experiments were performed at 77 K using a Coulter Omnisorp 100 gas analyzer. The specific surface area, $S_{BET}$, was determined from the linear part of the BET plot ($P/P_0$ = 0.05−0.15). The pore size distribution (PSD) was calculated from the adsorption branch using the KJS (Kruk−Jaroniec−Sayari) method.[14] The pore volume, $V$, was determined as the volume of liquid nitrogen adsorbed at a relative pressure of 0.995. The pore wall thickness ($b$) was calculated using $b = a - w_{KJS}$, where $a$ and $w_{KJS}$ are the unit cell dimension and pore size, respectively.

Quantitative elemental analysis of C, H, and N was carried out on a Carlo Erba EA1100 CHNS elemental analyzer. The rhodium and phosphorus content of the dendrimer species were determined by Galbraith Laboratories using inductively coupled plasma (ICP) atomic emission spectrometry.

$^{13}$C and $^{31}$P CP/MAS solid-state NMR spectra were obtained on a Bruker ASX-200 instrument operating at 50.32 and 80.99 MHz, respectively, with a spinning rate of 5.0−6.0 kHz and a contact time 2 ms. [MeP$^+$Ph$_3$]Br$^-$ was used as internal standard. $^{29}$Si CP/MAS solid-state NMR spectra were also recorded on the same instrument operating at 39.75 MHz with a spinning rate of 5.0−6.0 kHz and a contact time 2 ms.

Fourier transform infrared spectra were obtained using a Shimadzu FTIR-8400s spectrometer equipped with a Specac Silver Gate (ZnSe crystal) single reflection attenuated total reflectance (ATR) system. Spectra were recorded from 600 to 4000 cm$^{-1}$ using a resolution of 4 cm$^{-1}$ and 150 scans. Thermogravimetric analysis experiments were carried out on a combined DSC-TGA (SDT 2960) from TA Instruments. Simultaneous DSC−TGA measurements were obtained under air flow (100 mL min$^{-1}$) at a uniform heating rate of 20 °C min$^{-1}$ from 25 to 1000 °C. Approximately 10−20 mg of sample was used for each experiment.

Hydroformylation of 1-Octene (Scheme 4**).** To a 300 mL stainless steel, stirred tank Parr reactor equipped with a pressure transducer and temperature control was added 50 mg of rhodium-containing catalyst (9.7 $\mu$mol Rh), cyclohexane (90 mL), 1-octene (0.1 mol, 11.2 g), and *m*-xylene (11.2 g) as internal standard. The reactor was sealed and flushed three times with carbon monoxide and then pressurized to 500 psi with carbon monoxide. The reactor was then further pressurized to 1000 psi with hydrogen to give a 1:1 ratio of CO/H$_2$ with a total pressure of 1000 psi. The reactor was stirred at 600 rpm at 70 °C. Samples were routinely taken and analyzed by means of GC and NMR.

## Results and Discussion

**Characterization Results.** X-ray diffraction was used to determine the structure of the silica mesophase before and after the surface modification reactions that are involved in preparing the dendrimer-supported materials. The XRD patterns shown in Figure 1 indicate that the materials exhibit two-dimensional hexagonal symmetry characteristic of a MCM-41 silica mesophase.[17] The dominant peak at 2$\theta$ = ca. 1.3°, attributable to the (100) diffraction peak hardly changed during the various surface modifications steps, indicating that the overall structure of the mesophase has been preserved. The unit cell dimension $a$ was found be constant at 7.8 ± 0.2 nm for all materials, including the unmodified MCM-41 silica. It was calculated using $a = d_{100}(2/\sqrt{3})$, where the interplanar spacing $d_{100}$ was determined using the Bragg equation.

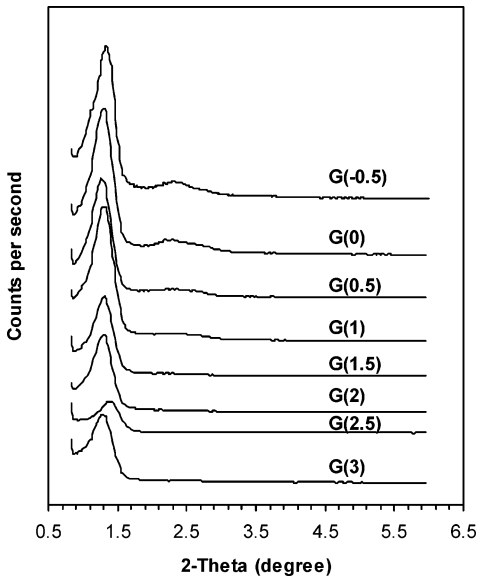


**Figure 1.** Powder X-ray diffraction patterns of MCM-41-supported dendrimers.

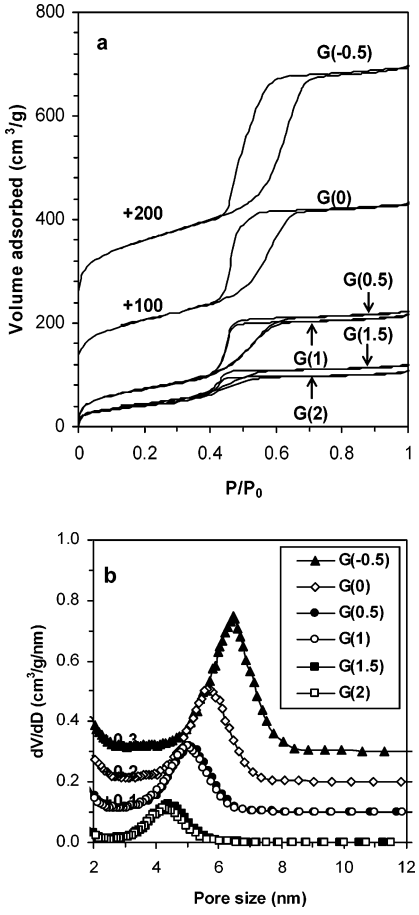


**Figure 2.** Nitrogen adsorption isotherms (a) and pore size distributions (b) for MCM-41-supported dendrimers.

Figure 2a,b depicts the nitrogen adsorption−desorption isotherms and the pore size distributions (PSD) for MCM-41 and the supported dendrimers. They are all of type IV isotherms and exhibit the condensation and evaporation steps characteristic of periodic mesoporous materials.[11,14,17] All the structural properties calculated

(17) Kresge, C. T.; Leonowicz, M. E.; Roth, W. J.; Vartuli, J. C.; Beck, J. S., *Nature* **1992**, *359*, 710.

**Table 1. Structural Properties of MCM-41-Supported Dendrimers**

| generation[a] | $S_{BET}$ ($m^2$/g) | $w_{KJS}$ (nm) | $b$ (nm)[b] | $V$[c] ($cm^3$/g) | $V/V_0$[d] expl | $V/V_0$[d] calcd |
|---|---|---|---|---|---|---|
| −0.5 | 585 | 6.5 | 1.12 | 0.77 | 1 | 1 |
| 0 | 390 | 5.6 | 2.25 | 0.51 | 0.71 | 0.74 |
| 0.5 | 271 | 5.0 | 2.97 | 0.34 | 0.56 | 0.59 |
| 1 | 265 | 5.0 | 2.79 | 0.33 | 0.54 | 0.59 |
| 1.5 | 157 | 4.3 | 3.49 | 0.18 | 0.34 | 0.44 |
| 2 | 145 | 4.2 | 3.59 | 0.16 | 0.30 | 0.42 |
| 2.5 | - | - | - | 0 | 0 | - |
| 3 | - | - | - | 0 | 0 | - |

[a] Generation (−0.5) refers to the MCM-41 support. [b] $b$ is the pore wall thickness. [c] $V$ is the pore volume of the material per g of silica. [d] $V_0$ is the pore volume of the starting material.

based on nitrogen adsorption data are shown in Table 1. It is instructive to note that the surface area, the pore volume, and pore size decrease significantly, but not linearly with increasing dendrimer generations. Compared to G(−0.5) material, i.e., pure MCM-41, the G(0), i.e., APTES-grafted MCM-41, exhibited significantly lower BET surface area (390 vs 585 $m^2$/g), pore volume (0.51 vs 0.78 $cm^3$/g), and pore size (5.6 vs 6.5 nm). This is consistent with similar observations reported in the literature.[18−20] Further decrease of the specific surface area and the pore volume and size took place upon reaction of methyl acrylate with G(0) material to obtain G(0.5). Compared to the starting material, the surface area and pore volume decreased by about 50%, whereas the pore size decreased by ca. 22%. However, as shown in Table 1, upon reaction of methyl propylaminopropionate-functionalized MCM-41 [G(0.5)] with ethylenediamine to obtain G(1) material, the structural properties hardly changed. This is most likely due to the fact that there is only a small difference in size between the half-generations and the next full generations, whereas the radius of the dendrimers changes significantly between full generations and the following half-generations. Thus, substantial decrease of $S_{BET}$, $V$, and $w_{KJS}$ takes place only during the branching steps. Consistent with this observation, the surface area, pore volume, and size of G(1.5) were much lower than those of G(1), but almost identical to those of G(2). As shown in Table 1, the thickness of the pore walls also increased stepwise, while remaining almost constant for materials containing grafted dendrimers corresponding to half-generations and the next full generation.

The values of the structural properties for G(2.5) and G(3) were not included in Table 1, as these samples did not adsorb any nitrogen, indicating that the pore system was completely blocked. Interestingly, the size of the grafted third-generation dendrimer, calculated on the basis of bond lengths, was found to be around 2.7−3 nm, which is approximately half of the pore size of the starting materials, i.e., 5.6 nm. This lends strong support to the fact that the pore systems for G(2.5) and G(3) materials are essentially blocked.

The behavior of the structural properties as a function of dendrimer generation provides clear evidence that the dendrimers grew inside the pore channels. However,

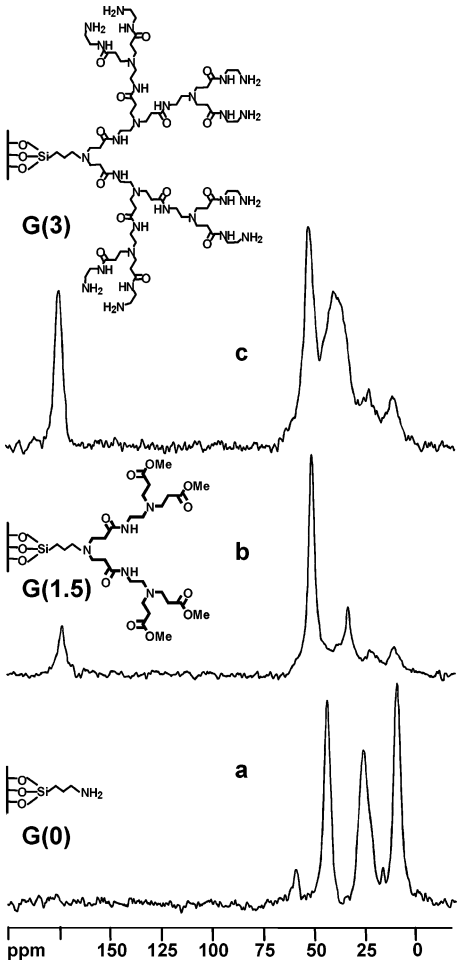


**Figure 3.** $^{13}C$ CP MAS NMR spectra.

based on strictly geometrical considerations, assuming that the organic modifier forms a "smooth" layer, the pore volume and the pore size of any two materials would be related by the following equation: $V_1/V_2 = (w_1/w_2)^2$. Using the starting material as a reference, the relative pore volumes for all samples were calculated using this equation and compared to the experimental data. As seen in Table 1, the actual pore volume decreased as a function of dendrimer generation faster than the calculated pore volume. Moreover, the difference between the experimental and calculated pore volume increased with dendrimer generation. Close scrutiny of literature data also indicates that upon surface modification of periodic mesoporous materials by organic species, the average pore size is often higher than $w_0(V/V_0)^{1/2}$, where $V$ is the pore volume of the modified material, and $V_0$ and $w_0$ are the pore volume and size of the starting material, respectively.[18−20] However, potential reasons for such behavior have not been explored.

Cross-polarized magic angle spinning (CP/MAS) $^{13}C$ NMR was used in this study for the identification of functional groups. Representative $^{13}C$ NMR spectra are shown in Figure 3. Figure 3a is the $^{13}C$ NMR for the aminopropylsilane-grafted MCM-41 [G(0)]. In this case, three peaks were obtained at 8.76, 25.34, and 43.35 ppm. They were attributed to the three carbons between the Si atom and the nitrogen, with increasing distance from the Si atom leading to a higher ppm value. There were also small peaks at 58.89 and 15.88 ppm, which

(18) Jaroniec, C. P.; Kruk, M.; Jaroniec, M.; Sayari, A. *J. Phys. Chem. B.* **1998**, *102*, 5503.
(19) Sayari, A.; Hamoudi, S. *Chem. Mater.* **2001**, *13*, 3151.
(20) Huang, H. Y.; Yang, R. T.; Chinn, D.; Munson, C. L. *Ind. Eng. Chem. Res.* **2003**, *42*, 2427.

can be attributed to small amounts of unhydrolyzed ethoxy groups attached to the Si atom. Figure 3b is the $^{13}C$ NMR of the G(1.5) species attached to the MCM-41. In this spectrum, five types of carbons can be identified. The peaks at 10.20, 22.23, and 32.88 ppm are again the three carbons of the original aminopropylsilane species that are slightly shifted due to the reactions that took place. The peak at 32.88 ppm also includes some of the carbons from the methacrylate moiety attached to the nitrogen at the branching points. This would explain the stronger intensity of this peak when compared to the other two peaks at 10.20 and 22.23 ppm. The peak at 50.61 ppm corresponds to the sum of two peaks attributable to the carbon atoms in two functional groups, namely the methoxy carbons of the ester functionalities as well as the carbons attached directly to nitrogen in the ethylenediamine species. The peak at 172.79 is due to the ester carbonyl carbons in the molecule. Figure 3c is the $^{13}C$ NMR spectrum of the G(3) dendrimer species attached to the surface of MCM-41. This spectrum shows the same general features, with the peaks at 51.74 and 39.45 ppm now similar in size. The two remaining carbons from the aminopropylsilane are barely visible at 10.58 and 21.98 ppm. This spectrum serves to show that the amide peaks at 173.51 ppm, although clearly visible and large, is subject to considerable line broadening and therefore does not allow for clear distinction between amide and ester groups (172.79 ppm) in the molecule. This is a limitation of the $^{13}C$ NMR technique, because the full generations were prepared by changing ester groups into amide groups and should therefore only contain amides. It is thus impossible to ascertain from $^{13}C$ NMR if full conversion between half-generations and full generations was accomplished. As shown below, FTIR spectroscopy was used to address this shortcoming.

The phosphinomethylated dendrimers were characterized by solid-state $^{31}P$ and $^{13}C$ NMR. The $^{13}C$ NMR spectra showed a new peak at 129 ppm corresponding to the aromatic carbons of the phosphine groups. A speak at −27 ppm in the $^{31}P$ NMR spectrum compares well with previously reported systems,[4] and the internal standard ($[MeP^+Ph_3]Br^-$) gave a peak at 20.71 ppm. After complexation, the $^{31}P$ NMR spectrum had two peaks, one at −27 ppm, corresponding to the uncomplexed phosphines, and the other at 26 ppm, corresponding to the rhodium-complexed phosphines.

Infrared spectroscopy proved to be a very useful technique to complement $^{13}C$ NMR data. The IR spectra for the support [G(−0.5)], grafted molecule [G(0)], and dendrimers [G(0.5)−G(3)] are shown in Figure 4. The absorption band at 1740 $cm^{-1}$, clearly visible in all the half-generations, was attributed to the CO stretching of the ester groups. The peaks at 1643 and 1547 $cm^{-1}$ were due to the CO stretching and the N−H bending/CN stretching of the secondary amide groups, respectively. It is therefore possible to distinguish between the amide function in the full-generation dendrimers and the ester function in the half-generations. Thus FTIR spectroscopy offers a simple tool to determine if the amidation reactions proceed to full conversion. However, FTIR does not provide any evidence as to whether the Michael additions proceed to completion or not. The FTIR spectrum of the G(0.5) species clearly shows the

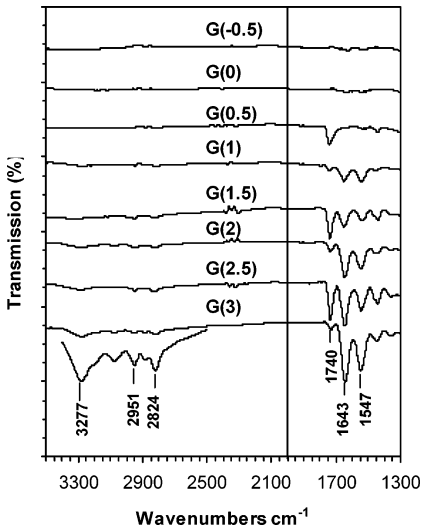


**Figure 4.** FTIR spectra for MCM-41-supported dendrimers.

ester incorporation, but at G(1), some ester functional groups can still be detected, even though the amides now represent the largest part of the functional groups. Then from G(1) to G(1.5), the incorporation of the ester groups is again clearly demonstrated. Likewise, at G(2), FTIR offered evidence of unreacted ester groups, and even up to G(3), a small amount of ester groups remained. It is instructive to note that the spectra were recorded using an ATR system that allows direct comparison between the samples due to the uniform contact of the sample with the ATR crystal. Therefore the increasing intensity of the peaks can be directly related to the amount of amides and esters in the samples. It is however difficult to quantify this increase exactly due to the increasing organic mass added to the MCM-41, and it is impossible to correct these spectra without using other information like silica content from TGA data. The TGA experiments will be discussed in the next section, but first there were other minor peaks in the IR spectra that deserve some mention. The peak at 3277 $cm^{-1}$ was assigned to the amide N−H stretching. The peaks at 2951 and 2824 $cm^{-1}$ were due to C−H stretching in the molecule.

Thermal analysis curves for representative samples are shown in Figure 5. From Figure 5A, it is clear that pristine MCM-41 lost weight between 25 and 121 °C. This event was associated with the desorption of water.[18] The rest of the curve (121−1000 °C) showed very slow, but continuous, weight loss. The weight loss between 121 and 800 °C was used as a baseline amount for the dendrimer-containing samples to correct for the weight loss of the silica in these samples. In Figure 5B, the DSC−TGA curve for the G(0) material was slightly different, as two large peaks were observed. There was still some water that desorbed completely by 121 °C. The second peak at about 325 °C was attributed to the pyrolysis of the aminopropyl group. This weight loss was accompanied by the release of a large amount of energy due to the strength of the carbon silicon bond. This conclusion was inferred from the DSC curve (Figure 5Bc) that shows a large exothermic peak at this point. In direct contrast to this, the DSC peak corresponding to the desorption of water shows that this event is slightly endothermic. In addition, the TGA peak at 325 °C had a large shoulder that extended to around 700

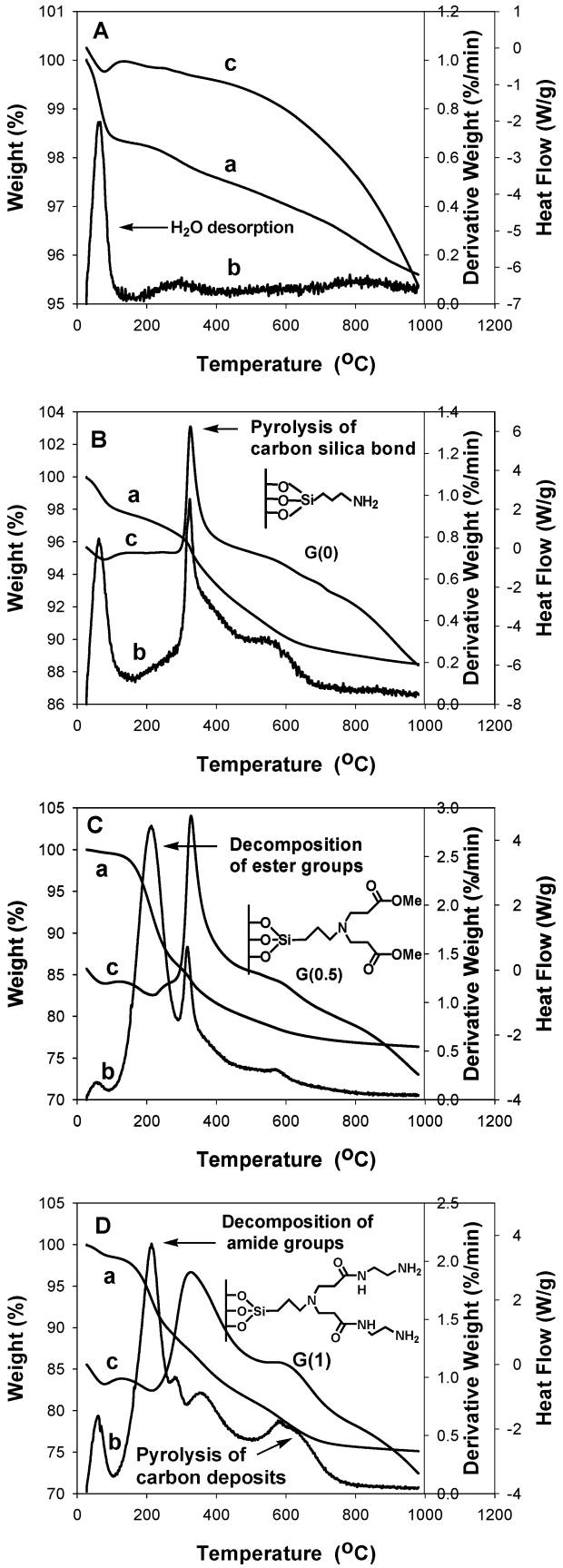


**Figure 5.** DSC−TGA data for MCM-41-supported dendrimers of different generations: (a) TGA curve, (b) derivative weight curve, (c) heat flow curve; (A) G(−0.5), MCM-41 support; (B) G(0); (C) G(0.5); and (D) G(1).

°C. This broad peak was attributed to further combustion of carbonaceous species (coke) that formed during

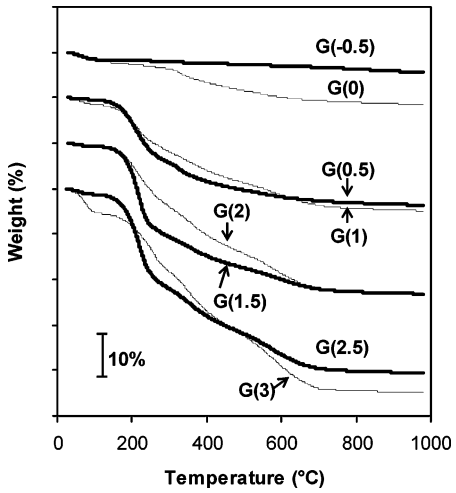


**Figure 6.** Weight loss as measured by TGA for MCM-41-supported dendrimers.

the pyrolysis of the aminopropyl species at 325 °C. This shoulder was observed in all the samples containing higher generation dendrimers. Thermogravimetric analysis data for the product of the double Michael addition to the G(0) MCM-41 species are shown in Figure 5C. In this case, a new peak was observed at about 210 °C in addition to the previous peaks associated with the water desorption and the pyrolysis of the aminopropyl group. The peak at 210 °C was attributed to the decomposition of the ester branches. Like the $H_2O$ desorption, this event was also endothermic, suggesting that decomposition, rather than pyrolysis, took place. A separate TGA experiment coupled with mass spectrometry (Pfeiffer ThermoStar instrument) lent further support to this contention. Indeed, the TGA peak at 210 °C was accompanied by the release of fragments of 55−60 and 85−86 amu, corresponding to the decomposition of the methyl acrylate species. At higher temperature, the formation of $CO_2$ was prevalent, indicative of the combustion of the remaining organic species.

Figure 5D shows the thermogravimetric analysis data for the G(1) material, which differs from the G(0.5) material (Figure 5C), only by the end group. As seen, the curves were very similar to those of the G(0.5) species with the amide decomposition giving a peak at 210 °C like the ester group in Figure 5C. This peak, however, had a shoulder at about 250 °C, which could be due to some ester groups remaining, as supported by FTIR data. In this case, a large shoulder at 600 °C was again observed and the high intensity of this peak could be due to the larger organic content of this material in comparison to the G(0) material.

The TGA spectra of the all the half-generations and full generations are represented together in Figure 6. It is clear that the half-generations and the next full generations exhibit similar behavior, indicating that the dendrimers are of similar molecular weights and, by inference, similar sizes. This is consistent with behavior of pore size and volume as determined by nitrogen adsorption (Figure 2, Table 1) and by the theoretical weight losses as shown in Table 2.

To assess the effectiveness of the reactions leading to different dendrimer generations, it is imperative to develop a methodology to accurately calculate the yield of such reactions. To this end, the DSC−TGA data were

**Table 2. Comparison between Experimental (TGA and Elemental Analysis) and Theoretical Weight Losses**

| | | | | weight loss (%) | | | |
|---|---|---|---|---|---|---|---|
| generation | %N | %C | %H | TGA (corrected) | elem anal. | theoretical | overall yield (%) |
| −0.5[a] | 0 | 0.15 | 0.73 | 0.00 | 0.00 | 0.00 | - |
| 0 | 1.72 | 4.59 | 1.67 | 7.00 | 7.34 | 7.13 | 98.16 |
| 0.5 | 1.45 | 11.49 | 2.18 | 20.94 | 21.75 | 23.33 | 89.74 |
| 1 | 4.03 | 11.73 | 2.6 | 21.22 | 20.20 | 27.45 | 77.29 |
| 1.5 | 3.31 | 16.55 | 2.88 | 30.81 | 30.30 | 45.45 | 67.79 |
| 2 | 5.7 | 16.98 | 3.71 | 30.63 | 29.39 | 49.54 | 61.83 |
| 2.5 | 5.28 | 21.1 | 3.96 | 37.99 | 40.53 | 65.42 | 58.07 |
| 3 | 7.36 | 19.59 | 4.32 | 37.95 | 35.33 | 68.68 | 55.26 |

[a] Generation −0.5 refers to the MCM-41 support.

used for the quantification of the growth of the dendrimers on the surface. This method was used earlier by Alper and co-workers,[6] but for this study, the approach was significantly refined by incorporating elemental analysis (EA) data and baseline correction. The EA was incorporated to first determine the amount of amines on the surface of the MCM-41 after grafting of APTES, i.e., G(0). This procedure is in our view more accurate and reproducible than previously used acid−base titration.[21] As shown in Table 2 (column 7), the EA data for the G(0) material allowed us to calculate the weight loss that would correspond to complete formation of dendrimers at every step of the synthesis. The actual weight loss corresponding to the combustion of supported dendrimers was determined by thermogravimetry as the weight loss between 121 and 800 °C, i.e., excluding the weight loss due to the desorption of water. This value was further corrected for the weight loss due to the amount of silica in the sample by using the weight loss of the unmodified MCM-41 silica support (Table 2, column 5). The weight losses for all materials were also calculated by adding the experimental amounts of C, N, and H obtained by EA and the amount of oxygen calculated on the basis of the theoretical oxygen-to-nitrogen ratio of any given dendrimer (Table 2, column 6). It is interesting to note that the obtained weight losses were consistent within 1−2% with corrected, TGA-derived weight losses (Table 2, column 6).

Assuming that all synthesis steps proceed with 100% yield, theoretical weight losses (Table 2, column 7) were calculated on the basis of the nitrogen content of material G(0). Comparison between the corrected experimental TGA weight loss and the theoretical weight loss allowed us to calculated the overall yield (OY) for each dendrimer generation (Table 2, column 8). It is seen that as the dendrimer generation increases, the OY decreases to reach 55.26 for the G(3) species. Although better than our previous results,[6] this may seem, at first glance, disappointing. However, a closer inspection of the statistics of dendrimer growth shows otherwise. At issue is the determination of the average yield (AY) per reaction (i.e., synthesis step) based on the overall yield, which represent a cumulative yield of all the steps involved. To address this question, let us consider the synthesis of G(3) material. The G(3) dendrimer was obtained from G(0) via 28 reaction steps. The following relationship holds: $OY = (AY)^x$, where $x$ is the number of reactions involved. Thus, $AY = (OY)^{1/x}$.

**Table 3. ICP Analysis of Rh and P**

| generation | P (%) | Rh (%) | generation | P (%) | Rh (%) |
|---|---|---|---|---|---|
| P-G(0) | 2.41 | | P-G(2) | 2.12 | |
| Rh-G(0) | 1.65 | 1.81 | Rh-G(2) | 1.81 | 0.619 |
| P-G(1) | 1.90 | | P-G(3) | .370 | |
| Rh-G(1) | 2.02 | 0.830 | | | |

In the case of the current G(3) dendrimer, $AY = (0.5526)^{1/28} = 0.979$. This shows that although the OY for the dendrimer at G(3) is only 55.26%, it is probably as good as is attainable in the divergent dendrimer synthesis approach without purification, and with all the steric interactions involved.[22]

This finding obviously means that some reactions did not go to completion, and it is believed that the largest hindering factor is the steric interference involved, especially for reactions with the higher dendrimers. Some evidence for this can be seen in the IR study, where residual ester functionalities were found in all the full-generation dendrimers.

Compared to amorphous silica, the current large-pore MCM-41 silica showed a higher degree of growth and higher yield of formation of grafted dendrimers.[6] Further dendrimer growth may be achieved by using even larger pore silicas such as SBA-15,[23] silica foam,[24] and pore-expanded MCM-41.[25,26]

**Phosphinomethylation and Complexation of the Different Generations.** The different generations were phosphinomethylated as described earlier. To carry out further metal complexation, it was imperative to determine the amount of phosphine that was incorporated into the material. To this end, an internal standard method in conjunction with $^{31}P$ NMR measurements was used. This afforded a close approximation of the phosphine content. To determine the phosphine levels more precisely, we used ICP analysis (Table 3). Although useful, the NMR method was less precise than the ICP analysis, but the results nonetheless could be used to determine the amount of rhodium for the complexation. This final synthesis step was achieved by reacting the rhodium-containing metal complex with the phosphinomethylated dendrimer (2 equiv of phosphine for each metal) species under argon in toluene. It is interesting to note that at this point our initial observation of the steric interaction of the dendrimer branches became very important. From the data it is clear that the G(0) and G(1) species incorporated much more phosphine and metal than the G(2) and G(3) species. Actually, the G(3) complexation was not even attempted due to the fact that almost no phosphine was present, even after 48 h of phosphinomethylation. This clearly supports our previous findings that the steric encumbrance of the higher generations has a detrimental effect on the phosphinomethylation and metal complexation.[3,6] Therefore, all reactions of higher generations of the dendrimers were critically affected by the space available for the reacting species. With the growth of the

(21) Tsubokawa, N.; Ichioka, H.; Satoh, T.; Hayashi, S.; Fujiki, K. *React. Funct. Polym.* **1998**, *37*, 75.

(22) Tomalia, D. A.; Naylor, A. M.; Goddard, W. A., III. *Angew. Chem., Int. Ed. Engl.* **1990**, *29*, 138.

(23) Zhao, D.; Huo, Q.; Feng, J.; Chmelka, B. F.; Stucky, G. D. *Science* **1998**, *279*, 548.

(24) Schmidt-Winkel, P.; Lukens, W. W., Jr.; Zhao, D.; Yang, P.; Chmelka, B. F.; Stucky, G. D. *J. Am. Chem. Soc.* **1999**, *121*, 254.

(25) Sayari, A.; Kruk, M.; Jaroniec, M.; Moudrakovski, I. L. *Adv. Mater.* **1998**, *10*, 1376.

(26) Sayari, A. *Angew. Chem., Int. Ed.* **2000**, *39*, 2920.

**Table 4. Comparison of the Activity for the Hydroformylation of 1-Octene of Rh-Complexed MCM-41-Supported Dendrimers with Different Generations[a]**

| generation | time (h) | conversion (%) | B:L[c] | TOF[b] ($h^{-1}$) |
|---|---|---|---|---|
| 0 | 8 | >99 | 1:1.6 | 1800 |
| 1 | 22 | >99 | 1:1.7 | 1430 |
| 2 | 20 | trace | - | - |

[a] Conditions: 50 mg of catalyst, 100 mmol of 1-octene, 70 °C, 1000 psi $H_2$:CO 1:1 in cyclohexane (90 mL). [b] TOF refers to average turnover frequency. [c] Branched to linear aldehyde.

**Table 5. Recycle Study of Rh-Complexed MCM-41-Supported G(0) Dendrimer[a]**

| substrate | cycle | conversion (%) | B:L | TOF[b] ($h^{-1}$) |
|---|---|---|---|---|
| 1-octene | 1 | >99 | 1:1.5 | 486 |
| 1-octene | 2 | >99 | 1:1.6 | - |
| 1-octene | 3 | >99 | 1:1.4 | - |

[a] Conditions: 22 h, 30 mg of catalyst, 50 mmol of substrate, 70 °C, 1000 psi $H_2$:CO 1:1 in cyclohexane (90 mL). [b] TON = 11 000.

dendrimers in a support with well-defined pore structure, we are able to determine when the saturation point is reached and can therefore now design supports to accommodate the desired degree of dendrimer growth.

**Catalytic Activity for the Hydroformylation of Olefins.** The catalytic properties of G(0)−G(2) materials were investigated using the hydroformylation of olefins as a test reaction. Among other substrates, a long chain linear olefin was used in the hydroformylation test reaction due to the specific separation challenges facing industrial processes of these olefins. The separation becomes challenging due to the high boiling point of long chain aldehyde products, and homogeneous catalysts of these olefins should not only be temperature stable but very robust as distillation is usually used to separate catalyst and product streams. A simple separation by filtration would have significant impact on the hydroformylation of these olefins. 1-Octene was selected as the olefin of choice and remarkable activity was observed with the current catalysts. The G(0) catalyst gave a turnover frequency (TOF) of over 1800 $h^{-1}$ at 70 °C with a total turnover number (TON) of 21 000. The TOF of this catalyst is significantly higher than our previous results (200 $h^{-1}$) where the TOF for styrene hydroformylation was determined at 70 °C over an amorphous silica-supported dendrimer catalyst (styrene is usually more reactive than 1-octene for the hydroformylation reaction).[4] In contrast, the selectivity to linear aldehyde was below expectations, with the best results giving a linear:branched selectivity of around 1.6 (Table 4). However, it was possible to recycle the catalysts three times before the amount of collected catalyst became too small to carry out further reaction cycles (Table 5). Moreover, several solvent systems were tested, and cyclohexane was found to be the best solvent to use in the recycle reactions. The G(1) catalyst was less active due to the lower levels of rhodium, and from G(2), the incorporation of metal was too low to give significant activity (Table 4). As shown in Table 6, the best catalyst, G(0), was also tested with other substrates and gave good results with styrene and vinyl acetate, particularly at 70−75 °C.

**Table 6. Activity in the Hydroformylation Reaction for the Rh-Complexed MCM-41-Supported G(0) Dendrimer[g]**

| substrate | amount (mmol) | *T* (°C) | conversion (%)[d] | B:L[e] | TOF ($h^{-1}$) |
|---|---|---|---|---|---|
| styrene | 10 | 75 | 99 | 9 | 345 |
| styrene | 10 | 60 | 40 | 12 | 138 |
| styrene | 10 | 50 | 25 | 15 | 86 |
| vinyl acetate | 5 | 80 | 57 | 11 | 98 |
| vinyl acetate | 10 | 75 | 60 | 12 | 206 |
| vinyl acetate | 10 | 60 | 50 | 11 | 173 |
| vinyl acetate | 10 | 50 | trace | nd | - |
| vinyl acetate | 10[a] | 25 | trace | nd | - |
| phenyl vinyl sulfone | 1 | 75 | 25 | f | - |
| 1-octene | 100[b] | 70 | 99 | 1:1.4 | 896[c] |

[a] 48 h, 25 mg of catalyst. [b] 35 mg of catalyst (5 $\mu$mol Rh), 24 h. [c] TON = 21 400. [d] Determined by GC. [e] Branched to linear aldehyde, determined by $^1$H NMR and GC. [f] No linear aldehyde detected. [g] Standard conditions: 22 h, 10 mg of catalyst (1.3 $\mu$mol of Rh) in $CH_2Cl_2$, 1000 psi $H_2$:CO 1:1.

## Conclusion

Polyamidoamine (PAMAM) dendrimers up to the third generation were grown for the first time inside the channels of a large-pore (6.5 nm) MCM-41 silica. Detailed characterization using nitrogen adsorption, solid state NMR, FTIR, thermogravimetry, and chemical analysis showed that the dendrimers formed inside the channels with an average yield higher than 97 %, all synthesis steps being included. The third generation was found to almost completely fill the pore system. Dendrimers of generations 0, 1, and 2 were phosphinomethylated and complexed with rhodium. The G(0) and G(1) materials were found to be excellent recyclable catalysts for olefin hydroformylation. A turnover frequency (TOF) as high as 1800 $h^{-1}$ was obtained for the hydroformylation of 1-octene at 70 °C.

**Acknowledgment.** A.S. is government of Canada Research Chair in *Catalysis using Nanostructured Materials*. We thank the Canada Foundation for Innovation (CFI), the Natural Sciences and Engineering Research Council (NSERC), and SASOL Technology (R & D) for financial support of this work. We also thank Mike Green at SASOL Technology for support, Tamer El Bokl for recording of DSC-TGA spectra, and Glenn Facey and Cheryl McDowall for recording of NMR spectra.

CM0493142